Table 4.2.4.3. *Mass attenuation coefficients ($cm^2\ g^{-1}$) (cont.)*

Radiation	Energy (MeV)	97 Berkelium	98 Californium
Ag $K\beta_1$	2.494E−02	6.66E+01	7.35E+01
Pd $K\beta_1$	2.382E−02	7.52E+01	8.24E+01
Rh $K\beta_1$	2.272E−02	8.51E+01	9.26E+01
Ag $K\bar{\alpha}$	2.210E−02	6.10E+01	6.92E+01
Pd $K\bar{\alpha}$	2.112E−02	1.03E+02	1.11E+02
Rh $K\bar{\alpha}$	2.017E−02	1.02E+02	1.25E+02
Mo $K\beta_1$	1.961E−02	1.25E+02	1.34E+02
Mo $K\bar{\alpha}$	1.744E−02	4.90E+01	5.00E+01
Zn $K\beta_1$	9.572E−03	1.86E+02	2.08E+02
Cu $K\beta_1$	8.905E−03	2.26E+02	2.49E+02
Zn $K\bar{\alpha}$	8.631E−03	2.46E+02	2.70E+02
Ni $K\beta_1$	8.265E−03	2.77E+02	3.01E+02
Cu $K\bar{\alpha}$	8.041E−03	3.52E+02	3.60E+02
Co $K\beta_1$	7.649E−03	3.57E+02	3.66E+02
Ni $K\bar{\alpha}$	7.472E−03	3.62E+02	3.86E+02
Fe $K\beta_1$	7.058E−03	4.22E+02	4.48E+02
Co $K\bar{\alpha}$	6.925E−03	4.43E+02	4.69E+02
Mn $K\beta_1$	6.490E−03	5.26E+02	5.52E+02
Fe $K\bar{\alpha}$	6.400E−03	5.92E+02	6.07E+02
Cr $K\beta_1$	5.947E−03	6.64E+02	6.87E+02
Mn $K\bar{\alpha}$	5.895E−03	6.78E+02	7.03E+02
Cr $K\bar{\alpha}$	5.412E−03	8.52E+02	8.71E+02
Ti $K\beta_1$	4.932E−03	1.09E+03	1.10E+03
Ti $K\bar{\alpha}$	4.509E−03	1.04E+03	1.05E+03

involve the use of filters, mirrors, and Laue and Bragg crystal monochromators, chosen so as to provide the best compromise between flux and spectral purity in a particular experiment. In other chapters, authors have discussed the use of techniques to improve the spectral purity of X-ray sources. This section does not purport to be a comprehensive exposition on the topic of filters and monochromators. Rather, it seeks to point the reader towards the information given elsewhere in this volume, and to add complementary information where necessary. A search of the Subject Index will find references to filters and monochromators that are not explicitly mentioned in the text of this section.

The ability to select photon energies, or bands of energies, depends on the scattering power of the atoms from which the monochromator is made and the arrangement of the atoms within the monochromator. The scattering powers of the atoms and their dependence on the energy of the incident photons were discussed in Sections 4.2.3 and 4.2.4 and are discussed more fully in Section 4.2.6. In brief, the scattering power of the atom, or *atomic scattering factor*, is defined, for a given incident photon energy, as the ratio of the scattering power of the atom to that of a free Thomson electron. The scattering power is denoted by the symbol $f(\omega, \Delta)$ and is a complex quantity, the real part of which, $f'(\omega, \Delta)$, is related to the elastic scattering cross section, and the imaginary part of which, $f''(\omega, \Delta)$, is related directly to the photoelectric scattering cross section and therefore the linear attenuation coefficient μ_l.

At an interface between, say, air and the material from which the monochromator is made, reflection and refraction of the incident photons can occur, as dictated by Maxwell's equations. There is an associated refractive index n given by

$$n = (1 + \chi)^{1/2}, \qquad (4.2.5.1)$$

where

$$\chi = -(r_e\lambda^2/\pi)\sum_j N_j f_j(\omega, \Delta), \qquad (4.2.5.2)$$

r_e is the classical radius of the electron, and N_j is the number density of atoms of type j.

An angle of total external reflection α_c exists for the material, which is a function of the incident photon energy, since $f_j(\omega, \Delta)$ is a function of photon energy. Thus, a polychromatic beam incident at the critical angle of one of the photon energies (E) will reflect totally those components having energies less than E, and transmit those components with energies greater than E. Fig. 4.2.5.1 shows calculations by Fukumachi, Nakano & Kawamura (1986) for the reflectivity of single layers of aluminium, copper and platinum as a function of incident energy for a fixed angle of incidence (0.2°). For the aluminium specimen, the reflectivity curve shows the rapid decrease in reflectivity as the critical angle is exceeded. The reflectivity in this region varies as E^{-2}. The effect of increasing atomic number can be seen: the higher the atomic factor $f(\omega, \Delta)$, the greater the energy that can be reflected from the surface. Also visible are the effects of the dispersion corrections $f'(\omega, \Delta)$ and $f''(\omega, \Delta)$ on reflectivity. For copper, the K shell is excited, and for platinum the $L_{\rm I}$, $L_{\rm II}$ and $L_{\rm III}$ shells are excited by the polychromatic beam.

Interfaces can therefore be used to act as low-pass energy filters. The surface roughness and the existence of impurities and contaminants on the interface will, however, influence the characteristics of the reflecting surface, sometimes significantly.

4.2.5.2. *Mirrors and capillaries*

Whilst neither of these classes of X-ray optical device is strictly speaking a monochromator, they nevertheless form component parts of monochromator systems in the laboratory and at synchrotron-radiation sources.

4.2.5.2.1. *Mirrors*

In the laboratory, mirrors are used in conjunction with conventional sealed tubes and rotating-anode sources, the emission from which consists of *Bremsstrahlung* upon which is superimposed the characteristic spectrum of the anode material (Subsection 2.3.5.2). The shape of the *Bremsstrahlung* spectrum can be significantly modified by mirrors, and the intensity emitted at harmonics of the characteristic wavelength can be

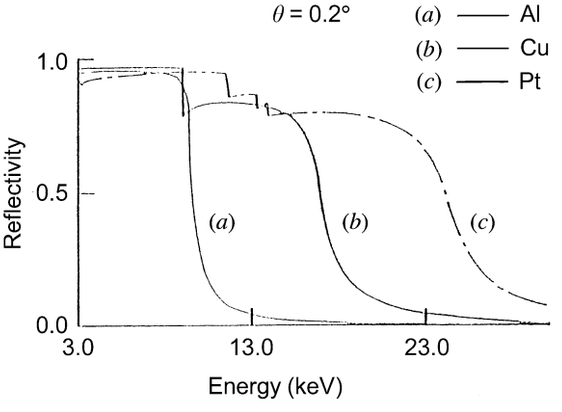

Fig. 4.2.5.1. The variation of specular reflectivity with incident photon energy is shown for materials of different atomic number and a constant angle of incidence of 0.2°. (*a*) Aluminium: note the rapid decrease of reflectivity with energy. (*b*) Copper: the sudden decrease of reflectivity is due to the modification of the scattering-length density owing to absorption at the K-absorption edge. (*c*) Platinum: the three discontinuities in the reflectivity curve are due to absorption at the $L_{\rm I}$-, $L_{\rm II}$-, and $L_{\rm III}$-absorption edges.

significantly reduced. More importantly, the mirrors can be fashioned into shapes that enable the emitted radiation to be brought to a focus. Ellipsoidal, logarithmic spiral, and toroidal mirrors have been manufactured commercially for use with laboratory X-ray sources. Since the X-rays are emitted isotropically from the anode surface, it is important to devise a mirror system that has a maximum angle of acceptance and a relatively long focal length.

At synchrotron-radiation sources, the high intensities that are generated over a very broad spectral range give rise to significant heat loading of subsequent monochromators and therefore degrade the performance of these elements. In many systems, mirrors are used as the first optical element in the monochromator, to reduce the heat load on the primary monochromator and to make it easier for the subsequent monochromators to reject harmonics of the chosen radiation. Shaped mirror geometries are often used to focus the beam in the horizontal plane (Subsection 2.2.7.3). A schematic diagram of the optical elements of a typical synchrotron-radiation beamline is shown in Fig. 4.2.5.2. In this, the primary mirror acts as a thermal shunt for the subsequent monochromator, minimizes the high-energy component that may give rise to possible harmonic content in the final beam, and acts as a vertical collimator. The radii of curvature of mirrors can be changed using a mechanical four-point bending system (Oshima, Harada & Sakabe, 1986). More recent advances in mirror technology enable the shape of the mirror to be changed through use of the piezoelectric effect (Sussini & Labergerie, 1995).

4.2.5.2.2. *Capillaries*

Capillaries, and bundles of capillaries, are finding increasing use in situations where a focused beam is required. The radiation is guided along the capillary by total external reflection, and the shape of the capillary determines the overall flux gain and the uniformity of the focused spot. Gains in flux of 100 and better have been reported. There is, however, a degradation in the angular divergence of the outgoing beam. For single capillaries, applications are laboratory-based protein crystallography, microtomography, X-ray microscopy, and micro-X-ray fluorescence spectroscopy. The design and construction of capillaries for use in the laboratory and at synchrotron-radiation sources has been discussed by Bilderback, Thiel, Pahl & Brister (1994), Balaic & Nugent (1995), Balaic, Nugent, Barnea, Garrett & Wilkins (1995), Balaic *et al*. (1996), and Engström, Rindby & Vincze (1996). They are usually used after other monochromators in these applications and their role as a low-pass energy filter is not of much significance.

Bundles of capillaries are currently being produced commercially to produce focused beams (ellipsoidally shaped bundles) and half-ellipsoidal bundles are used to form beams of large cross section from conventional laboratory sources (Peele *et al.*, 1996; Kumakov & Komarov, 1990).

4.2.5.2.3. *Quasi-Bragg reflectors*

For one interface, the reflectivity (R) and the transmissivity (T) of the surface are determined by the Fresnel equations, *viz*:

$$R = \left|(\theta_1 - \theta_2)/(\theta_1 + \theta_2)\right|^2, \qquad (4.2.5.3)$$

and

$$T = \left|2\theta_1/(\theta_1 + \theta_2)\right|^2, \qquad (4.2.5.4)$$

where θ_1 and θ_2 are the angles between the incident ray and the surface plane and the reflected ray and the surface plane, respectively.

If a succession of interfaces exists, the possibility of interference between successively reflected rays exists. Parameters that define the position of the interference maxima, the line breadths of those maxima, and the line intensity depend *inter alia* on the regularity in layer thickness, the interface surface roughness, and the existence of surface tilts between successive interfaces. Algorithms for solving this type of problem are incorporated in software currently available from a number of commercial sources (Bede Scientific, Siemens, and Philips). The reflectivity profile of a system having a periodic layer structure is shown in Fig. 4.2.5.3. This is the reflectivity profile for a multiple-quantum-well structure of alternating aluminium gallium arsenide and indium gallium arsenide layers (Holt, Brown, Creagh & Leon, 1997). Note the interference maxima that are superimposed on the Fresnel reflectivity curve. From the full width at half-maximum of these interference lines, it can be inferred that the energy discrimination of the system, $\Delta E/E$, is 2%. The energy range that can be reflected by such a multilayer system depends on the interlayer thickness: the higher the photon energy, the thinner the layer thickness.

Commercially available multilayer mirrors exist, and hitherto they have been used as monochromators in the soft X-ray region in X-ray fluorescence spectrometers. These monochromators are typically made of alternating layers of tungsten and carbon, to maximize the difference in scattering-

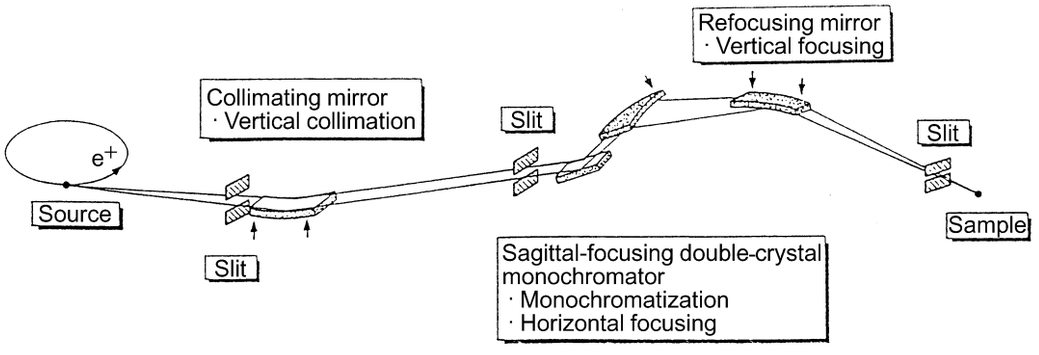

Fig. 4.2.5.2. The use of mirrors in a typical synchrotron-radiation beamline. The X-rays are emitted tangentially to the orbit of the stored positron beam. They pass through a beam-defining slit onto a mirror that serves three purposes, *viz* energy discrimination, heat absorption, and focusing, by means of a mechanical four-point bending system. The beam then passes into a double-crystal monochromator, which selects the desired photon energy. The second element of this monochromator is capable of being bent sagittally using a mechanical four-point bending system to focus the beam in the horizontal plane. The beam is then refocused and redirected by a second mirror.